THE JOURNAL OF BIOLOGICAL CHEMISTRY
Vol. 279, No. 45, Issue of November 5, pp. 46810–46817, 2004

Printed in U.S.A.

Active Site Engineering of the Epoxide Hydrolase from *Agrobacterium radiobacter* AD1 to Enhance Aerobic Mineralization of *cis*-1,2-Dichloroethylene in Cells Expressing an Evolved Toluene *ortho*-Monooxygenase*

Received for publication, July 6, 2004, and in revised form, August 18, 2004
Published, JBC Papers in Press, August 30, 2004, DOI 10.1074/jbc.M407466200

Lingyun Rui‡, Li Cao‡, Wilfred Chen§, Kenneth F. Reardon¶, and Thomas K. Wood‡‖

From the ‡Departments of Chemical Engineering and Molecular and Cell Biology, University of Connecticut, Storrs, Connecticut 06269–3222, the §Department of Chemical and Environmental Engineering, University of California, Riverside, California 92521, and the ¶Department of Chemical Engineering, Colorado State University, Fort Collins, Colorado 80523-1370

Chlorinated ethenes are the most prevalent groundwater pollutants, and the toxic epoxides generated during their aerobic biodegradation limit the extent of transformation. Hydrolysis of the toxic epoxide by epoxide hydrolases represents the major biological detoxification strategy; however, chlorinated epoxyethanes are not accepted by known bacterial epoxide hydrolases. Here, the epoxide hydrolase from *Agrobacterium radiobacter* AD1 (EchA), which enables growth on epichlorohydrin, was tuned to accept *cis*-1,2-dichloroepoxyethane as a substrate by accumulating beneficial mutations from three rounds of saturation mutagenesis at three selected active site residues, Phe-108, Ile-219, and Cys-248 (no beneficial mutations were found at position Ile-111). The EchA F108L/I219L/C248I variant coexpressed with a DNA-shuffled toluene *ortho*-monooxygenase, which initiates attack on the chlorinated ethene, enhanced the degradation of *cis*-dichloroethylene (*cis*-DCE) an infinite extent compared with wild-type EchA at low concentrations (6.8 μM) and up to 10-fold at high concentrations (540 μM). EchA variants with single mutations (F108L, I219F, or C248I) enhanced *cis*-DCE mineralization 2.5-fold (540 μM), and EchA variants with double mutations, I219L/C248I and F108L/C248I, increased *cis*-DCE mineralization 4- and 7-fold, respectively (540 μM). For complete degradation of *cis*-DCE to chloride ions, the apparent V_{max}/K_m for the recombinant *Escherichia coli* strain expressing the EchA F108L/I219L/C248I variant was increased over 5-fold as a result of the evolution of EchA. The EchA F108L/I219L/C248I variant also had enhanced activity for 1,2-epoxyhexane (2-fold) and the natural substrate epichlorohydrin (6-fold).

Epoxide hydrolases (EH)[1] (EC 3.3.2.3) hydrolyze an epoxide to its corresponding vicinal diol by the addition of a water molecule (1). In mammalian systems, epoxides are frequently found as intermediates in the catabolic pathways of various xenobiotics, including unsaturated aliphatic and aromatic hydrocarbons (2–4). These intermediates are potentially harmful as the oxirane moiety of epoxides is electrophilically reactive and can form adducts with various cellular components including DNA, RNA, proteins, and other small molecules (5, 6); hence, it is vital for the biological system to detoxify these reactive species. Together with the conjugation reaction catalyzed by glutathione *S*-transferases, conversion of epoxides by EHs into chemically and toxicologically less active diols constitutes the major mechanism for detoxification in mammalian systems (5).

Although mammalian EHs have been extensively studied for detoxification, interest in microbial EHs has arisen primarily because of the potential of the enzymes as enantioselective biocatalysts (1, 7, 8). It is also of interest to investigate the detoxification role of microbial EHs and genetically adapt this universally successful detoxification strategy to the process of aerobic, cometabolic biodegradation of chlorinated ethenes in which toxic epoxides form as the primary intermediates (6). Chlorinated ethenes, such as trichloroethylene (TCE) and *cis*-1,2-dichloroethylene (*cis*-DCE), constitute a large group of priority pollutants (126 chemicals from the U.S. Clean Water Act) (9, 10). Because they are toxic, it is critical to remediate these compounds (11). Whereas reductive dechlorination of chlorinated ethenes under anaerobic conditions has the risk of accumulation of the well known carcinogen, vinyl chloride (11–14), aerobic co-metabolic mineralization (conversion to chloride ion) of these compounds by microorganisms expressing various nonspecific oxygenases suffers from the inability of the cell to detoxify the reactive chlorinated epoxyethanes that are the primary metabolites (6). The chlorinated epoxyethanes may cause covalent modification of cellular components, inactivation of enzymes, and even cell death and thus greatly limit the extent of transformation (6, 15–18).

Recently, a novel glutathione *S*-transferase from *Rhodococcus* sp. strain AD45 having activity toward *cis*-1,2-dichloroepoxyethane (*cis*-DCE epoxide) was coexpressed with an evolved toluene *ortho*-monooxygenase (TOM), TOM-Green, in *E. coli* in our laboratory. It showed significant detoxification of the reactive epoxide intermediates from *cis*-DCE, *trans*-1,2-dichloroethylene, and TCE (19) (Fig. 1). TOM is a three-component, diiron enzyme encoded by the *Burkholderia cepacia* G4 genes *tomA012345* (20), catalyzing hydroxylation of toluene to form 3-methylcatechol through the intermediate *o*-cresol (21). TOM also oxidizes TCE primarily to Cl^- and CO_2 *in vivo* (22, 23) and

* This work was supported by National Science Foundation Grants BES-9911469 and BES-0331416. The costs of publication of this article were defrayed in part by the payment of page charges. This article must therefore be hereby marked "*advertisement*" in accordance with 18 U.S.C. Section 1734 solely to indicate this fact.

‖ To whom correspondence should be addressed. Tel.: 860-486-2483; Fax: 860-486-2959; E-mail: twood@engr.uconn.edu.

[1] The abbreviations used are: EH, epoxide hydrolase; TCE, trichloroethylene; DCE, dichloroethylene; TOM, toluene *ortho*-monooxygenase; Kan, kanamycin; GC, gas chromatography; AnEH, *Aspergillus niger* epoxide hydrolase; EchA, epoxide hydrolase from *Agrobacterium radiobacter* AD1.

aerobically degrades various other chlorinated ethenes (20, 24, 25). TOM-Green originated from the first DNA shuffling of a non-heme monooxygenase and has enhanced activity for both TCE degradation and naphthalene oxidation due to a single amino acid substitution, V106A, in TomA3 (26).

In contrast to glutathione *S*-transferases, which require glutathione as the cofactor for their enzymatic activity (27), EHs do not require a cofactor (1). Unfortunately, there are no EHs of microbial origin known to have activity toward chlorinated epoxyethanes. Nevertheless, a number of microorganisms contain EHs with various substrate ranges (28–32), and various directed evolution and rational protein engineering techniques may be used to alter enzymatic activity (33, 34). Hence, it was investigated here whether an epoxide hydrolase could be tuned to accept chlorinated epoxyethanes as a substrate.

The EH from *Agrobacterium radiobacter* AD1 (EchA, GenBank™ accession number Y12804) (35) was chosen for protein engineering because its physiological substrate, epichlorohydrin (2-chloropropylene oxide), resembles chlorinated epoxyethanes. EchA (294 amino acids) contains a core domain with typical α/β hydrolase fold topology formed by an eight-stranded β-sheet sandwiched by α-helices and an α-helical cap domain protruding from the core domain (36). The catalytic triad residues Asp-107, Asp-246, and His-275 are located in a hydrophobic internal cavity between the two domains (36). The catalytic reaction follows a two-step mechanism involving an alkyl-enzyme ester intermediate, which is further hydrolyzed via the attack of a water molecule (36, 37).

We reasoned that the substrate range of the enzyme may be tailored to accept a chlorinated epoxyethane based on the three-dimensional structure of EchA (PDB accession code 1EHY) (36), an understanding of the molecular level properties of this enzyme (36), and its relatedness to similar EH enzymes (2, 38) and haloalkane dehalogenase (DhlA) (39, 40). Saturation mutagenesis was used rather than site-directed mutagenesis to introduce all possible mutations at one site to explore a larger fraction of the protein sequence space (41). This is the first report of targeted mutagenesis of epoxide hydrolases at these positions, of an epoxide hydrolase with activity toward chlorinated epoxyethanes, and of enhancement of *cis*-DCE degradation by combining an evolved monooxygenase and evolved epoxide hydrolase to detoxify the reactive intermediates.

EXPERIMENTAL PROCEDURES

Chemicals, Organisms, and Growth Conditions—All materials were of highest purity available and purchased from Fisher Scientific Company (Pittsburgh, PA) except for epichlorohydrin (Acros Organics, Morris Plains, NJ), betaine (Sigma), and *cis*-DCE (TCI America, Inc., Portland, OR). *E. coli* TG1 (42) was used for cloning and gene expression. Recombinant strains were routinely grown at 37 °C in Luria-Bertani (LB) broth (43) supplemented with kanamycin (Kan, 100 μg/ml) and chloramphenicol (Cam, 50 μg/ml) to maintain plasmids unless otherwise stated. All whole-cell experiments used LB + Kan + Cam cultures inoculated from single, fresh colonies; exponential phase cells were harvested at an optical density at 600 nm (A) of ~1.5. Isopropyl β-D-thiogalactopyranoside (IPTG, 0.5 mM) was used to induce TOM-Green that was under control of the *tac-lac*UV5 tandem promoter in plasmid pMMB206 (44) and also to induce EchA under control of the *lac* promoter in pBS(Kan) (26); IPTG was added at an A of 0.2–0.3 for 2 h. The exponentially grown cells were washed three times with one volume of Tris-HNO_3 buffer (50 mM, pH 7.0) to remove interfering byproducts and trace chloride (26).

Protein Analysis and Molecular Techniques—Total cellular protein for the exponentially growing culture was determined with the Total Protein kit (Sigma), and expression of recombinant proteins was analyzed with standard Laemmli discontinuous sodium dodecyl sulfate-12% polyacrylamide gels (SDS-PAGE) (43). Plasmid DNA was isolated using a Midi or Mini kit (Qiagen, Inc.), and polymerase chain reaction (PCR) products were purified with a Wizard® PCR Preps DNA purification system (Promega Corp., Madison, WI). DNA fragments were isolated from agarose gels using a QIAquick gel extraction kit (Qiagen, Inc.). *E. coli* was transformed using electroporation with a Gene Pulser/Pulse Controller (Bio-Rad) at 15 kV/cm, 25 μF, and 200 Ω.

TABLE I
Oligonucleotide primers used for saturation mutagenesis at positions Phe-108, Ile-111, Ile-219, and Cys-248 of EchA

Primer	Sequences
Phe-108 Front	AGGCGTACGTCGTTGGCCATGACNNNGCGGCCATC
Phe-108 Rear	TTATGGAGGACGATGGCCGCGNNNTCATGGCCAAC
Ile-111 Front	ACGTCGTTGGCCATGACTTCGCGGCCNNNGTCCTCC
Ile-111 Rear	ATGAATTTATGGAGGACNNNGGCCGCGAAGTCATG
Ile-219 Front	CTTCAACTACTATCGTGCCAACNNNAGGCCCGATG
Ile-219 Rear	ACAGAGCGGCATCGGGCCTNNNGTTGGCACGATAG
Cys-248 Front	ATATGGGGTTTGGGAGATACTNNNGTGCCCTATGC
Cys-248 Rear	TCAATGAGTGGAGCATAGGGCACNNNAGTATCTCC
EH Front[a]	AGCTATGACCATGATTACGCCAAGC
EH Rear[b]	CGTTGTAAAACGACGGCCAGTGA

[a] Utilizing the natural KpnI restriction site upstream of *echA*.
[b] Utilizing the natural SacI restriction site downstream of *echA*.

PCR Amplification and Plasmid Construction—To stably and constitutively express the EH from *A. radiobacter* AD1, the *echA* gene was amplified by PCR using plasmid pEH20 (35) as the template with the forward primer 5′-ATAGCGGTACCACAACGGTTTCCCT-3′ and reverse primer 5′-ATTGCTGTCGACCAGTCATGCTAGCC-3′, where underlining indicates the KpnI and SalI restriction enzyme sites, respectively. The PCR amplification was performed with *Pfu* DNA polymerase (Stratagene) using a PCR program of 30 cycles of 94 °C for 45 s, 55 °C for 45 s, 72 °C for 2 min, and a final extension of 72 °C for 10 min. The PCR fragment was double digested with KpnI and SalI and ligated into pBS(Kan) at the same restriction sites, yielding pBS(Kan)EH (Fig. 2).

The six genes, *tomA0-tomA5*, of TOM-Green were obtained from plasmid pBS(Kan)TOM-Green (26) after EcoRI and PvuI restriction digestion and purification from an agarose gel. The resulting 5345-bp fragment was ligated into pMMB206 after digestion with the same restriction enzymes, resulting in pMMB206-TOM-Green (Fig. 2).

Saturation Mutagenesis of EchA—A gene library encoding all possible amino acids at positions Phe-108, Ile-111, Ile-219, and Cys-248 of EchA in pBS(Kan)EH was constructed by replacing the target codon with NNN via overlap extension PCR (41). Four pairs of degenerate primers, Phe-108 Front/Phe-108 Rear, Ile-111 Front/Ile-111 Rear, Ile-219 Front/Ile-219 Rear, and Cys-248 Front/Cys-248 Rear (Table I) were designed to randomize codons Phe-108, Ile-111, Ile-219, and Cys-248 in the nucleotide sequence, respectively. Two additional primers for cloning were EH Front and EH Rear (Table I), which were upstream and downstream of the natural KpnI and SacI restriction sites flanking the *echA* gene (Fig. 2). To minimize random point mutations, *Pfu* DNA polymerase was used in the PCR. Addition of betaine (1 M) in the PCR mixture was used to improve the amplification of DNA by reducing the formation of secondary structure in the GC-rich region when necessary (45). In the first round of saturation mutagenesis, pBS(Kan)EH was used as the template, and mutagenesis was performed individually at sites Phe-108, Ile-111, Ile-219, and Cys-248. In the second round of mutagenesis, pBS(Kan)EH C248I (containing amino acid substitution Cys-248I in EchA) was used as the template and sites Phe-108 and Ile-219 were randomized individually. In the third round, pBS(Kan)EH F108L/C248I (containing amino acid substitutions F108L and C248I in EchA) was used as the template and site Ile-219 was subjected to saturation mutagenesis. Two degenerate PCR fragments were produced for each site with 463 and 749 bp for site Phe-108, 457 and 754 bp for site Ile-111, 800 and 414 bp for site Ile-219, and 853 and 327 bp for site Cys-248. After purifying from agarose gels, the two fragments for each site were combined at a 1:1 ratio as templates to obtain the full-length PCR product with the EH Front and EH Rear primers. The resulting randomized PCR product (1167 bp) was cloned into pBS(Kan)EH after double digestion with KpnI and SacI, replacing the corresponding fragment in the original plasmid.

Screening for Enhanced cis-DCE Degradation—Evolved EchA activity toward *cis*-DCE epoxide was found indirectly by monitoring the concentration of chloride ion released from *cis*-DCE epoxide (generated by TOM-Green oxidation of *cis*-DCE) degradation by the evolved EchA (Fig. 1). TG1 cells harboring plasmids pMMB206-TOM-Green and pBS(Kan)EH variants were grown in 96-well plates, washed three times with Tris-HNO_3 buffer (50 mM, pH 7.0), and contacted with shaking at 37 °C in an airtight chamber, 23 × 20 × 23 cm, with *cis*-DCE vapor (2 ml) for 18 h. The inorganic chloride ions generated from the mineralization of *cis*-DCE by whole cells were detected by adding 40 μl

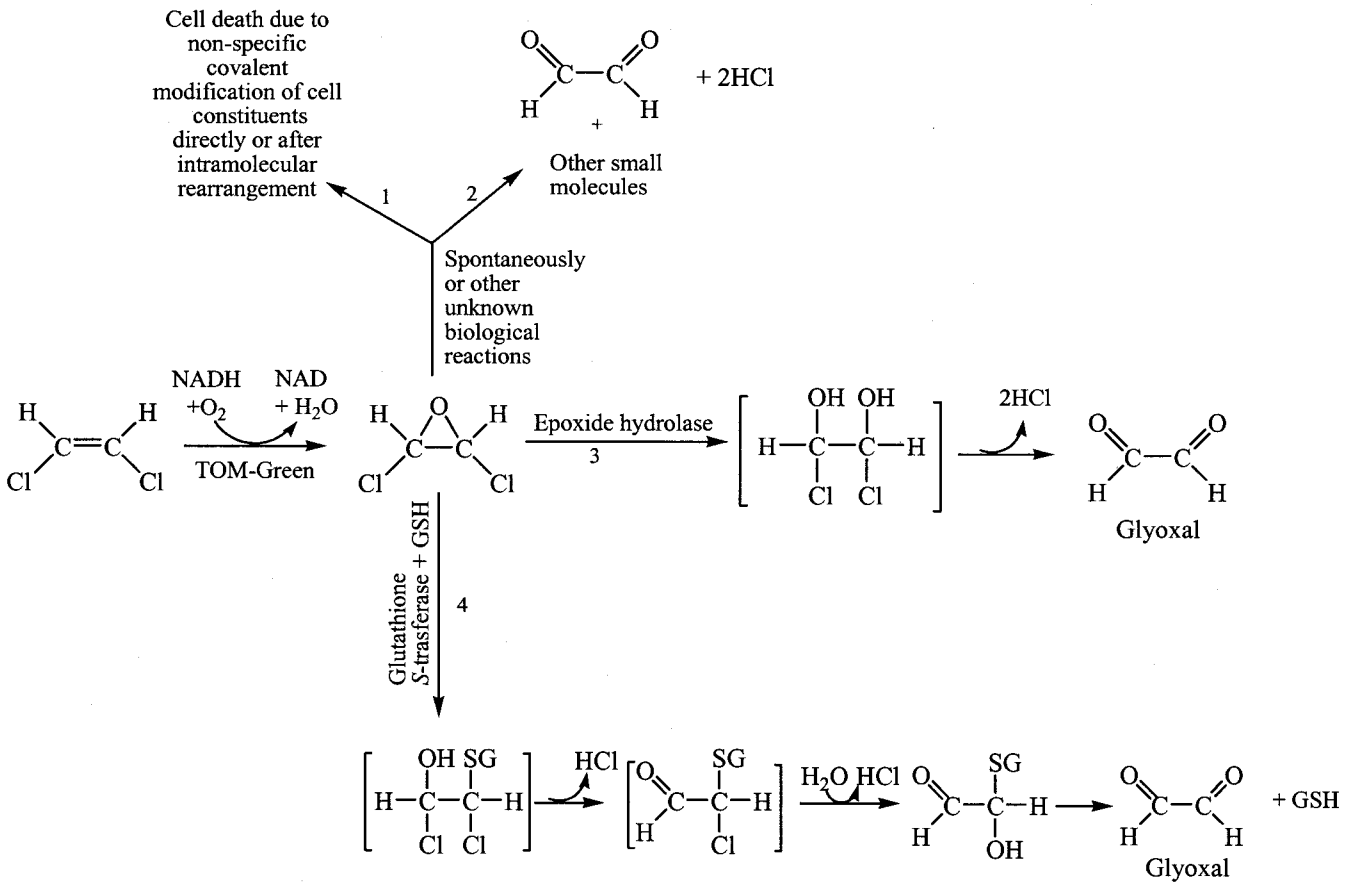

FIG. 1. **Metabolic engineering to enhance *cis*-DCE mineralization by cloning an evolved epoxide hydrolase along with an evolved toluene *ortho*-monooxygenase (TOM-Green) (adapted from van Hylckama Vlieg and Janssen; Ref. 6).** Steps 1 and 2 are the two possible spontaneous transformation pathways for *cis*-DCE epoxide. Steps 3 (this work) and 4 (19) represent two major detoxification strategies through which *cis*-DCE epoxide may be biologically converted by either an epoxide hydrolase or glutathione *S*-transferase (IsoILR1).

of 0.25 M $Fe(NH_4)(SO_4)_2$ in 9 M HNO_3 and 40 μl of saturated $Hg(SCN)_2$ in 95% ethanol to the 200 μl of supernatant in each well of the 96-well plate and measured at 450 nm (26).

Extent and Kinetics of cis-DCE Mineralization—For determining the extent of mineralization of *cis*-DCE (as indicated by Cl^- production) from the best colonies identified by the 96-well screening, the exponentially growing cells were washed three times with Tris-HNO_3 buffer (50 mM, pH 7.0). Then the cell suspension (2.5 ml) was adjusted to an A of 3, sealed in 15-ml glass serum vials, and contacted with *cis*-DCE at an initial liquid concentration of 540 μM (based on a Henry's Law constant of 0.17 (46)). 2.5 μmol of *cis*-DCE was injected into the cells in 5 μl of dimethyl formamide (DMF) at 0.2 vol%. Isopropyl β-D-thiogalactopyranoside (0.5 mM) was added along with 5 mM sodium succinate (as a substrate to produce NADH). After 2 h of incubation at 37 °C and 250 rpm, the whole-cell reaction was quenched by heating the vials in boiling water for 90 s and centrifuging (16,000 × *g*, 4 min) to collect the supernatant. Chloride ion concentrations in 500 μl of supernatant were measured spectrophotometrically at 460 nm as indicated above. Cells contacted with the same amount of DMF were used as the negative control, and at least three independent experiments were analyzed.

To determine the kinetics of *cis*-DCE mineralization, the A of the cell culture was 1.2, and the initial *cis*-DCE concentrations were 6.8 to 540 μM (using different stock solutions of 6.25, 25, 125, and 500 mM in DMF at 0.2–0.4 vol%). The supernatant chloride ion concentrations generated from mineralizing *cis*-DCE for each concentration were measured at 9 min for 6.8 and 13.5 μM, 15 min for 27 μM, 21 min for 54 μM, 38 min for 135 μM, 56 min for 270 μM, and 67 min for 540 μM. The contacting times were varied to detect significant Cl^- while maintaining the mineralization rate in the linear range for each *cis*-DCE concentration. Parallel experiments determining the *cis*-DCE degradation rate were conducted using gas chromatography (GC) to monitor *cis*-DCE depletion as described previously (25). Headspace samples from the same cell suspensions contacted with *cis*-DCE at various concentrations in the *cis*-DCE kinetics experiments were analyzed before the cells were quenched to determine Cl^- production.

Purification of EchA—Both wild-type EchA and variant F108L/I219L/C248I were expressed in TG1/pBS(Kan) for enzyme purification, and the method of Rink *et al.* (35) was adopted with modification. Exponentially growing precultures were diluted 1:100 in 3 liters of fresh Luria-Bertani broth containing 100 μg/ml Kan and incubated with shaking at 37 °C. Isopropyl β-D-thiogalactopyranoside (1 mM) was added when the cell A reached 0.3, and the culture was incubated at 25 °C overnight with aeration. Cells were harvested, washed by centrifugation at 10,000 × *g*, 4 °C for 10 min with TEMAG buffer (10 mM Tris-SO_4, 1 mM EDTA, 1 mM β-mercaptoethanol, 0.02% sodium azide, and 10% glycerol, pH 7.5), and resuspended in 30 ml of the same buffer. Cells were disrupted by a French® pressure cell press (Spectronic Instruments, Rochester, NY) and centrifuged at 20,000 × *g*, 4 °C for 30 min. Anion exchange was performed by applying 30 ml of the supernatant to 30 ml of DEAE-Sepharose (Sigma) (47), and proteins were eluted with a continuous gradient ammonium sulfate in TEMAG (0–1 M). Fractions with the highest enzymatic activity were pooled and dialyzed against TEMAG buffer overnight at 4 °C and were further purified via size exclusion chromatography by adding 1.5 ml to 80 ml of Sephacryl S-100 HR (Sigma). Fractions with purified EchA (with the highest EH activity and the highest purity as visualized on SDS-PAGE) were pooled and dialyzed against TEMAG buffer overnight. The final product was stored at −20 °C with glycerol (10% v/v) for future use; variant F108L/I219L/C248I and wild-type enzyme were purified from 10% to 80 and 90%, respectively. Activity of column fractions was determined using a polypropylene 96-well plate format with styrene oxide (5 mM) as the substrate rather than the reported epichlorohydrin (35). Column fractions (10 μl) were added to 136 μl of TE buffer and incubated with 5 mM styrene oxide at 37 °C for 15 min, followed by the sequential addition of 100 mM 4-nitrobenzylpyridine (75 μl) and triethylamine (75 μl). The chromogenic reaction of styrene oxide with 4-nitrobenzylpyridine was measured at 620 nm with a Multiskan reader (Fisher Scientific), and disappearance of the blue color indicated the disappearance of styrene oxide.

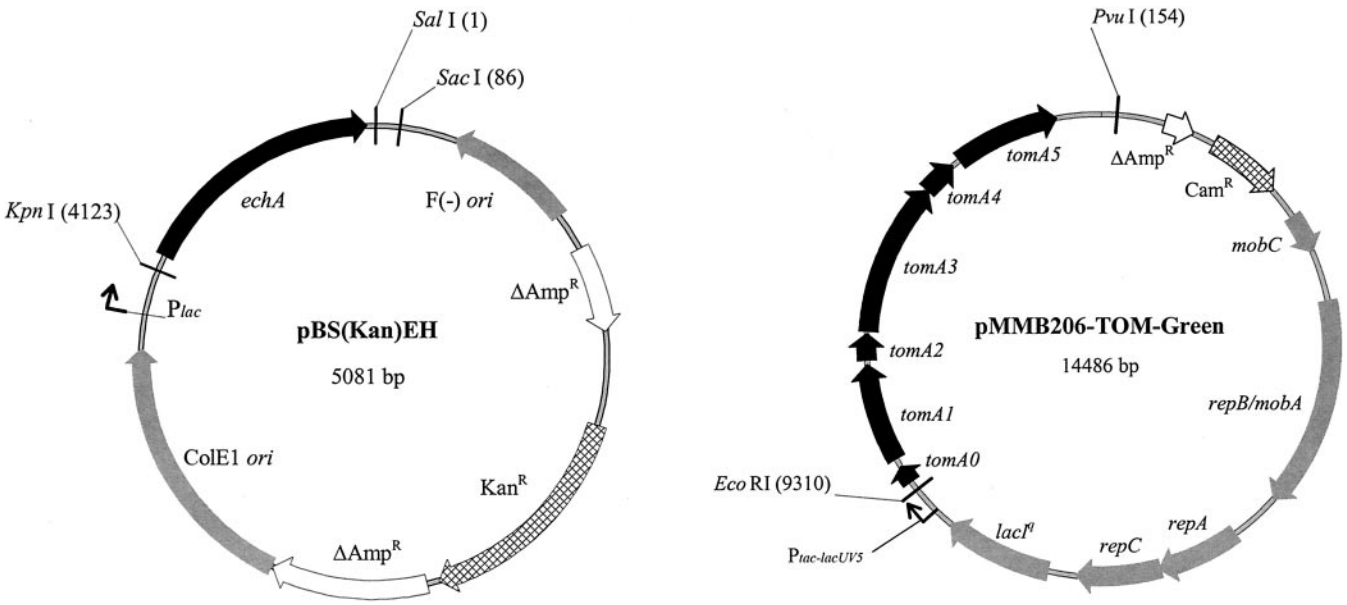

FIG. 2. **Plasmid maps of pBS(Kan)EH and pMMB206-TOM-Green.** Cloning restriction enzyme sites are shown. TOM-Green is a variant of toluene *ortho*-monooxygenase from DNA shuffling with the substitution V106A in *tomA3* (26).

EH Assays—As a preliminary assay, whole cells of TG1/pBS(Kan)EH (grown in Luria-Bertani broth + 100 μg/ml Kan) were tested for EchA activity in *E. coli* using a chromogenic reaction of the epoxide epichlorohydrin with 4-nitrobenzylpyridin (35). The assay was performed in 1.5-ml microcentrifuge tubes with 100 μl of exponentially grown cells contacted with 10 mM epichlorohydrin in 400 μl of TE buffer (50 mM Tris-SO_4, 1 mM EDTA, pH 9.0) for around 1 h at room temperature. 250 μl of 4-nitrobenzylpyridine (100 mM in 80 vol% ethylene glycol and 20 vol% acetone) was then added, the cells were heated at 80 °C for 10 min, and 250 μl of triethylamine (1:1 in acetone) was added. The blue color was proportional to the remaining epichlorohydrin. Purified enzyme (2.5 μg) was also tested at 5 mM epichlorohydrin at 37 °C for 30 min and with 4-nitrobenzylpyridine heated at 50 °C for 30 min.

EchA-specific activity was also determined with whole cells using the substrate 1,2-expoxyhexane. Cells prepared the same way as for the *cis*-DCE mineralization experiments (2.5 ml with contact A ~2.0) were sealed in 15-ml glass vials and used for the assay, and headspace concentrations of 1,2-expoxyhexane (5 mM) were determined by monitoring headspace samples with GC. The GC (Agilent 6890 series) was equipped with a 0.10% AT-1000 packed column (Alltech, length 1.829 m, inner diameter 3.175 mm, film thickness 2.159 mm) and a flame-ionization detector (FID). The FID was supplied with hydrogen (30 ml/min) and air (300 ml/min), and nitrogen was used as the carrier gas (20 ml/min). Headspace samples injected into the GC every 15 min were analyzed isothermally at 200 °C; the retention time of 1,2-expoxyhexane was 1.7 min under such conditions. TG1/pMMB206-TOM-Green/pBS(Kan) was used as the negative control.

To determine the specific activity of purified EchA toward 1,2-expoxyhexane, 1 or 20 μg EchA was added to 2.5 ml of Tris-HCl buffer (50 mM, pH 7.4) in a sealed 15-ml glass vial and reacted with 0.025 to 5 mM 1,2-expoxyhexane. The activity was determined using GC by monitoring substrate depletion with headspace samples injected every 15 min (same GC conditions as with the whole-cell experiments). The Henry's Law constant for 1,2-epoxyhexane was estimated as 0.089 using extraction with ethyl acetate.

TOM-Green Activity and DNA Sequencing—To ensure relatively constant TOM-Green activity during *cis*-DCE degradation with the various EchA variants, parallel, whole-cell naphthol synthesis assays were conducted by incubating the same cells that were used for *cis*-DCE degradation with naphthalene in the absence of *cis*-DCE to monitor TOM-Green activity as described previously using tetrazotized *o*-dianisidine and a spectrophotometric assay (26). A dye terminator cycle sequencing protocol based on the dideoxy method of sequencing DNA developed by Sanger *et al.* (48) was used to sequence both strands of wild-type and mutant EchA (49).

Homology Structural Modeling—The three-dimensional coordinates of the EchA variants were generated with SWISS-MODEL Server (50–52) using a structure model of wild-type EchA as the template (36) and visualized with Swiss-PdbViewer (50–52). The use of the structural model instead of the original x-ray structure of EchA as the structural template for homology modeling was because the x-ray structure was obtained from an inactive enzyme, possibly with false crystal packing forces, which resulted in one of the catalytic triad residues, Asp-246, being positioned outside of the active site (36). Here we used the EchA structure model with the loop containing Asp-246 rebuilt in the more likely active conformation of EchA (36) because it represents a common picture of active site α/β hydrolase-fold enzymes (36) and was further confirmed by mutagenesis studies (37).

RESULTS

Plasmid Construction—To create clone libraries via electroporation and reliably screen them for enhanced EH activity, a stable plasmid that expresses EchA constitutively, pBS(Kan)EH (Fig. 2), was constructed that utilizes a constitutive *lac* promoter and kanamycin resistance gene. Use of kanamycin circumvents segregational instability and avoids feeder colonies that are associated with ampicillin resistance vectors. The resulting epoxide hydrolase expressed in *E. coli* TG1 had activity toward its natural substrate epichlorohydrin (10 mM) based on the preliminary EH assay using 4-nitrobenzylpyridine (data not shown). TOM-Green was expressed from pMMB206-TOM-Green (Fig. 2), a wide host range, low copy number vector that is compatible with pBS(Kan)EH.

Saturation Mutagenesis, Screening, and Sequencing Analysis—Saturation mutagenesis was performed individually on the four EchA sites, Phe-108, Ile-111, Ile-219, and Cys-248, which we chose based on their close vicinity to the catalytic triad residues (Asp-107, Asp-246, and His-275; Fig. 3) (36). Two of these residues, Phe-108 and Cys-248, were hypothesized previously to influence substrate binding in this or a related enzyme, although mutagenesis was not performed at these sites (2, 36). By cloning DNA fragments from saturation mutagenesis back into the corresponding position of pBS(Kan)EH, all possible amino acids were introduced at the three sites, respectively. A library containing ~2,000 colonies for each site was obtained. About 300 of those colonies were screened in 96-well plates for *cis*-DCE degradation because 292 independent clones from saturation mutagenesis at one site need to be screened for a 99% probability that each possible codon has been tested (49).

Whole cells expressing the EchA variants and TOM-Green with enhanced *cis*-DCE mineralization, as indicated by in-

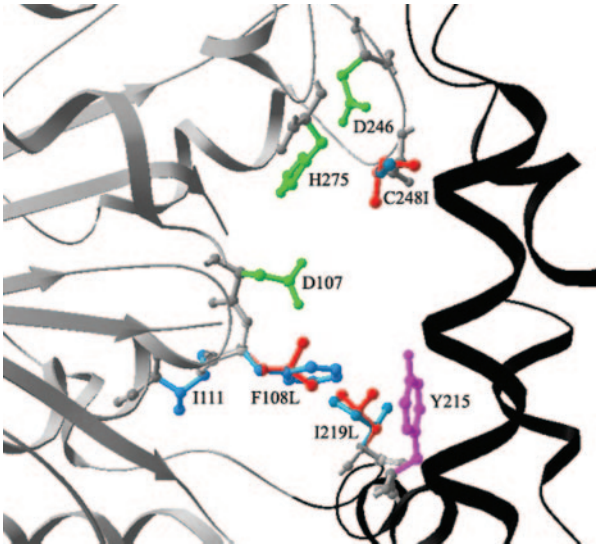

FIG. 3. **Active site of EchA F108L/I219L/C248I based on homology structural modeling.** The catalytic triad residues Asp-107, Asp-246, and His-275 (*green*) are located in a predominantly hydrophobic internal cavity between the core domain (*gray*) and the cap domain (*black*). The three amino acid substitutions, Leu-108, Leu-219, and Ile-248 (*red*), are superimposed on the wild-type residues, Phe-108, Ile-219, and Cys-248 (*blue*). Tyr-215 (*purple*), a proton-donor residue, has van der Waals contact with Ile-219.

creased Cl^- released, were found from three of the mutagenesis libraries. The beneficial amino acid substitutions were F108L, I219F, and C248I, indicating each of these positions is important for adapting EchA to the substrate *cis*-DCE epoxide (Table II). No beneficial amino acid substitution was found at position Ile-111. Although the three variants enhanced *cis*-DCE mineralization to a similar extent when co-expressed with TOM-Green (2.4- to 2.7-fold; Table II), the C248I mutation was slightly superior so it was used as a new template for a second round of saturation mutagenesis to combine the beneficial mutations at positions Phe-108 and Ile-219. Saturation mutagenesis, rather than site-directed mutagenesis, was used to introduce the new residues at these positions because it was not clear how the three altered residues would interact.

Around 300 colonies from each of the two resulting libraries were again screened for improved *cis*-DCE mineralization activity using 96-well microtiter plates. The beneficial mutations that resulted in further improvements in *cis*-DCE mineralization from the two libraries were F108L/C248I (7.1-fold) and I219L/C248I (4.2-fold). As EchA F108L/C248I enhanced *cis*-DCE mineralization more than EchA I219L/C248I, it was used as the new template for a third round of saturation mutagenesis at position Ile-219. The same size library was screened, and four positive variants were found, all containing I219L. Thus, the best EchA variant for enhancing *cis*-DCE mineralization was created by three rounds of saturation mutagenesis with amino acid substitutions F108L, I219L, and C248I. The mutation I219F that was discovered in the first round of saturation mutagenesis as beneficial was lost in the further mutagenesis experiments, indicating I219F might not be compatible with other mutations at Cys-248 and/or Phe-108. The whole process shows that beneficial mutations can be quickly accumulated by multiple rounds of saturation mutagenesis and screening relatively small libraries.

Enhanced cis-DCE Mineralization by the Evolved EchA—As *cis*-DCE epoxide is commercially unavailable and short-lived with a half-life of 72 h (16), *cis*-DCE mineralization was used as the indirect assay to characterize evolved EchA. In evaluating *cis*-DCE mineralization, TOM-Green in pMMB206-TOM-Green was always expressed to initiate the degradation reaction by forming *cis*-DCE epoxide. Because the mineralization of *cis*-DCE is the concerted reaction by both TOM-Green and EchA, whole cells were used. Naphthol synthesis assays were used to monitor TOM-Green activity in the *cis*-DCE degradation experiments of EchA mutants F108L/C248I and F108L/I219L/C248I to ensure the difference in *cis*-DCE mineralization rate was not caused by differences in TOM-Green activity. It was assumed that EchA should have no effect on naphthol formation, either because no naphthalene epoxide was formed during the TOM-Green transformation or because naphthalene epoxide (if formed) was not within the substrate range of EchA. TOM-Green activity was relatively constant with each EchA isoform (Table III) at ~1 nmol/min·mg protein at 0.24 mM naphthalene.

In addition, the EchA expression levels of all the mutants listed in Table II were characterized using SDS-PAGE (41). The TOM-Green α (size 54.4 kDa) and β (size 37.7 kDa) subunits were clearly seen as well as EchA (34 kDa), and the expression levels were the same for all the EchA mutants as well as for TOM-Green (data not shown). Hence, the enhancements in *cis*-DCE activity were not because of changes in protein expression.

The enhancements in *cis*-DCE mineralization at 540 μM initial substrate concentration by whole cells expressing TOM-Green and the EchA variants created in the first, second, and third rounds of saturation mutagenesis are listed in Table II. In comparing the enhancement of *cis*-DCE mineralization by EchA variant to the wild-type, the part of *cis*-DCE mineralized by TOM-Green alone (in TG1/pMMB206-TOM-Green/pBS-(Kan)) was subtracted as background signal as no EchA was involved. Table II shows that there was only a slight increase in *cis*-DCE mineralization rate by wild-type EchA compared with the $EchA^-$ strain, indicating that *cis*-DCE epoxide is a poor substrate of wild-type EchA. Although the single mutation variants at the three separate sites (Phe-108, Ile-219, and Cys-248) did not result in a large enhancement in *cis*-DCE mineralization, the combination of beneficial mutations did lead to a step-by-step improvement and finally brought about 10-fold enhancement in *cis*-DCE mineralization rate with the variant containing the triple mutations F108L/I219L/C248I (Table II). As the cell systems are isogenic and there were equivalent EchA protein expression levels and similar TOM-Green activity, these results indicate that the EchA mutants, especially F108L/I219L/C248I, were tailored to accept *cis*-DCE epoxide within their substrate range and to participate in the biological degradation of *cis*-DCE epoxide generated as the primary intermediate by TOM-Green.

Kinetics of cis-DCE Mineralization by the Best EchA Variant—EchA F108L/I219L/C248I co-expressed with TOM-Green was further characterized for enhancement in *cis*-DCE mineralization rate at different substrate concentrations, and the saturation constants, apparent V_{max} and apparent K_m, for the co-expression system were obtained (Table III). Whole cells expressing EchA variant F108L/I219L/C248I had enhanced *cis*-DCE mineralization at all the substrate concentrations, with the largest difference at lower *cis*-DCE concentrations (6.8–27 μM) as there was no detectable activity with wild-type EchA below 25 μM. This was reflected by 40% reduction in the apparent K_m with EchA F108L/I219L/C248I. Thus, EchA F108L/I219L/C248I not only elevated the apparent V_{max} for *cis*-DCE mineralization but also increased the affinity toward *cis*-DCE.

Although we expected an enhancement in the *cis*-DCE degradation rate as well (initial disappearance rate), the parallel experiments monitoring *cis*-DCE degradation via GC did not

TABLE II

Enhanced cis-DCE mineralization by whole cells expressing EchA variants after saturation mutagenesis at sites Phe-108, Ile-219, and Cys-248

Strain TG1/pMMB206-TOM-Green/pBS(Kan)EH was used to simultaneously express EchA (wild-type and mutants) and TOM-Green.

Enzyme	Mineralization rate of *cis*-DCE[a,b,c]		Chloride ion release in 2 h[c]		
	Rate	-Fold increase[d]	Cl^-	Mineralization	-Fold increase[d]
	nmol/min·mg protein		*μM*	*%*	
EchA$^-$[e]	2.35 ± 0.23		357 ± 24	17.8	
Wild-type EchA	2.88 ± 0.25	1.0	420 ± 34	21.0	1.0
F108L	3.60 ± 0.56	2.4	519 ± 45	26.0	2.6
I219F	3.72 ± 0.61	2.6	544 ± 54	27.2	3.0
C248I	3.78 ± 0.22	2.7	548 ± 7	27.4	3.0
I219L/C248I	4.55 ± 0.67	4.2	606 ± 24	30.3	4.0
F108L/C248I	6.13 ± 0.48	7.1	898 ± 137	44.9	8.7
F108L/I219L/C248I	7.57 ± 0.21	9.9	1036 ± 37	51.8	10.9

[a] Determined via chloride ion release after 2 h of contact (compare Table III with 67 min of contact).
[b] Total protein: 0.18 mg protein/ml·A.
[c] Initial *cis*-DCE concentrations was 540 μM calculated based on Henry's Law with Henry's constant 0.17 (46). 1 mM were added as if all the volatile organic was in the liquid phase.
[d] Strains expressing EchA variants compared to that of wild-type EchA after subtracting the chloride generated by TG1/pMMB206-TOM-Green/pBS(Kan) (no epoxide hydrolase control).
[e] EchA$^-$: TG1/pMMB206-TOM-Green/pBS(Kan).

TABLE III

Kinetics of cis-DCE mineralization by whole cells expressing the best EchA variant, F108L/I219L/C248I, their activity toward 1,2-epoxyhexane, and TOM-Green activity via naphthalene oxidation

Enzyme[a]	Mineralization rate of *cis*-DCE, nmol/min·mg protein[b,c,d]							Kinetics of *cis*-DCE mineralization		1,2-Epoxyhexane hydrolysis rate	Naphthol formation rate
	6.8 μM	13.5 μM	27 μM	54 μM	135 μM	270 μM	540 μM	Apparent V_{max}	Apparent K_m		
								nmol/min·mg protein	*μM*	*nmol/min·mg protein*[c,e]	*nmol/min·mg protein*[c,f]
EchA$^-$	1.1 ± 0.2	2.5 ± 0.1	2.7 ± 0.1	3.5 ± 0.1	3.4 ± 0.4	4.4 ± 0.8	4.5 ± 0.5	4.5	13	0	0.97 ± 0.09
Wild-type EchA	0.2 ± 0.2	2.6 ± 0.3	3.1 ± 0.1	4.5 ± 0.2	5.2 ± 0.7	4.8 ± 0.0	5.4 ± 0.4	5.4	14	118 ± 12	1.03 ± 0.02
F108L/I219L/C248I	4.4 ± 1.1	8.7 ± 0.3	11.1 ± 1.4	11.3 ± 0.5	13.3 ± 1.8	11.4 ± 0.5	11.0 ± 0.2	13.3	8.1	253 ± 18	0.91 ± 0.04

[a] EchA$^-$: TG1/pMMB206-TOM-Green/pBS(Kan); wild-type EchA: TG1/pMMB206-TOM-Green/pBS(Kan)EH; F108L/I219L/C248I: TG1/pMMB206-TOM-Green/pBS(Kan)EH F108L/I219L/C248I.
[b] Determined via chloride ion release after 67 min of contact time (compare Table II with 2 h of contact time).
[c] Total protein was 0.18 mg protein/(ml·A).
[d] Initial *cis*-DCE concentrations were calculated based on Henry's Law with a Henry's constant of 0.17 (46).
[e] Determined via gas chromatography by monitoring 1,2-epoxyhexane degradation using whole cells (5 mM initial concentration).
[f] Naphthalene was added at 5 mM although its solubility is 0.24 mM in water (54).

show a significant difference in the initial degradation rates between the strains with wild-type EchA and the F108L/I219L/C248I variant (data not shown). For example, at an initial liquid *cis*-DCE concentration of 135 μM, about 55% *cis*-DCE was consistently depleted within 38 min for both strains. However, for the F108L/I219L/C248I variant, the degraded *cis*-DCE was almost completely mineralized as indicated by the Cl^- production, whereas only 36% of the degraded *cis*-DCE was mineralized with wild-type EchA. As the two strains are isogenic with only three amino substitutions, the enhanced Cl^- formation arises from the additional conversion route of *cis*-DCE epoxide by the evolved EchA (Fig. 1).

Enhanced 1,2-Epoxyhexane and Epichlorohydrin Hydrolysis—To obtain direct evidence that the EchA isoforms were functionally expressed in the system, EH activity toward an epoxide was examined. Though *cis*-DCE epoxide would be the best substrate for this study, it is commercially unavailable and difficult to synthesize and utilize (16), so 1,2-epoxyhexane, a good substrate of wild-type EchA (35), was chosen as the alternative substrate to determine EH activity of wild-type EchA, EchAF108L/C248I, and EchA F108L/I219L/C248I. The same whole-cell system used for the *cis*-DCE mineralization experiments, TG1/pMMB206-TOM-Green/pBS(Kan)EH, was used for determining EH activity. For whole cells, there was a 2.1-fold increase in the 1,2-epoxyhexane activity by EchA F108L/I219L/C248I compared with the wild-type enzyme (Table III). To corroborate these results, purified EchA was tested, and the k_{cat} for 1,2-epoxyhexane hydrolysis with the F108L/I219L/C248I variant and wild-type enzymes were 8.4/sec and 3.6/sec, respectively (K_m values of 43 and 20 μM, respectively). Hence, there was activity enhancement similar to that obtained with whole cells. Further, the increase in the 1,2-epoxyhexane hydrolysis rate seemed to follow the same trends as the enhancement in *cis*-DCE mineralization: a gradual increase was seen as the beneficial mutations were combined, as indicated by the intermediate activity of the dual mutant EchA F108L/C248I toward 1,2-epoxyhexane (156 ± 20 nmol/min·mg protein with whole cells). A 6-fold improvement in epichlorohydrin hydrolysis was also obtained using purified enzymes (94 ± 8 μmol/min·mg for the F108L/I219L/C248I variant *versus* 16 ± 2 μmol/min·mg for the wild-type enzyme). Hence, EchA was optimized for more than just *cis*-DCE epoxide by the three mutations.

DISCUSSION

It is clearly shown in this report that by active site engineering at carefully selected residues (EchA Phe-108, Ile-219, and Cys-248) and by accumulating beneficial mutations via saturation mutagenesis, EchA was engineered to accept *cis*-DCE epoxide as a substrate. This is significant because the aerobic biodegradation of chlorinated ethenes requires the detoxification of the reactive epoxides formed as the primary intermediates after oxygenase attack. To our knowledge, this is the first report of protein engineering of epoxide hydrolases at these or analogous sites for any application.

For the rational redesign of EchA, the important residues must first be identified. The choice of sites here was based on the investigation of the active site of EchA and structural

comparison with other related enzymes, including the haloalkane dehalogenase from *Xanthobacter autotrophicus* (DhlA) (PDB accession code 2HAD) (39, 40), marine-soluble epoxide hydrolase (PDB accession code 1CQZ) (38), and *Aspergillus niger* epoxide hydrolase (AnEH, PDB accession code 1QO7) (2). The structural model of a human microsomal epoxide hydrolase based on AnEH was also considered (2). These enzymes contain the canonical α/β hydrolase fold with conserved catalytic triad (2), indicating their common phylogenic origin. However, there are many structural differences because of their low sequence homology (20–30% amino acid identity in the core region), which yields an extremely versatile substrate range (2). Based on the hypervariability at key structural residues that may contribute to the shape and substrate binding properties of the active site cavity (2, 36, 38, 39) and, in turn, might affect the substrate specificity, we altered the active site residues Phe-108 and Cys-248 of EchA for acceptance of a new chlorinated substrate.

Phe-108 is in close vicinity to the substrate (Fig. 3) as it is located next to the nucleophile Asp-107, which initiates the hydrolysis reaction by attacking the substrate (36), and contributes to the formation of the structurally conserved oxyanion hole, which is needed to stabilize the negatively charged transition state occurring in hydrolysis (36). In addition, Phe-108 has been suggested to be involved in substrate binding (36). Despite its structural and functional importance, the equivalent residues of Phe-108 in the related enzymes vary considerably, with Trp-125 in DhlA (39), Trp-227 in human microsomal EH (2), Trp-334 in marine liver cytosolic EH (38), Ile-193 in AnEH (2), and Phe-108 in EchA (36).

Cys-248 is one residue away from the catalytic acidic residue Asp-246 (36). Its equivalent residue in AnEH, Cys-350, is a constituent of the active site wall and was proposed to contribute to the geometry and character of the active site cavity (2). In addition, the side chain of Leu-262, the equivalent residue in DhlA, appears to block the tunnel that connects the active site cavity with the outside solvent region (39). Cys-248 is also a hypervariant codon with the equivalent residues in other related enzymes as Cys-350 in AnEH (2), Phe-406 in human microsomal EH (2), Val-497 in cytosolic EH (38), and Leu-262 in DhlA (39). We reasoned that mutating Cys-248 may have subtle effects on the specificity and reactivity of the enzyme.

Although there is no evidence showing that Ile-219 interacts directly with substrate during the reaction nor has it been previously identified as influencing catalytic activity, we determined that it has van der Waals contact with both Phe-108 and Tyr-215 (within 4 Å; Fig. 3). Tyr-215 was suggested to function as the proton donor in the catalytic mechanism of EchA (53) and was thought to direct initial substrate binding and positioning in the active center (2). As this Tyr residue role is conserved in other EHs (2), direct mutation at this residue could cause drastic changes in the active site properties, whereas we reasoned that mutation at Ile-219, which interacts with Tyr-215, could bring some subtle, beneficial effects. Change in the side chain of Ile-219 was thought to bring slight changes in the position or orientation of Tyr-215 as well as Phe-108 and, in turn, could influence substrate binding.

We also tried saturation mutagenesis at position Ile-111 as it is also in the vicinity of one of the catalytic residues, Asp-107 (Fig. 3), and seems to be a hypervariant residue with Phe-128 in DhlA (39), Phe-196 in AnEH, and Leu-230 in microsomal EH (2). However, we did not obtain any variant with enhanced *cis*-DCE mineralization when coexpressed with TOM-Green; hence, its role may be more structural than catalytic.

Concerted effects from the changes of the three residues (F108L/I219L/C248I) may optimize the size, shape, and hydrophobic character of the active site to facilitate binding and stabilization for *cis*-DCE epoxide and its transitional state intermediates. Interestingly, engineering EchA for the poor substrate *cis*-DCE epoxide also improved activity for both 1,2-epoxyhexane (Table III) and epichlorohydrin. Hence, the substrate specificity of EchA may be extended further to epoxides of other chlorinated ethenes, such as TCE and tetrachloroethylene, by protein rational design or directed evolution. Further, in combination with metabolic pathway engineering, the chlorinated epoxyethanes may be channeled into productive metabolic pathways, potentially allowing chlorinated ethenes to be utilized as a sole carbon and energy source, since the inability of various chlorinated ethenes to support growth is not because of lack of energy during conversion (6) but because no suitable enzyme system is able to harvest the energy.

Acknowledgments—We thank Prof. Dick Janssen for the gift of plasmid pEH20 and Prof. Bauke Dijkstra (both of the University of Groningen) for the EchA structure model. We thank Ying Tao of the Wood laboratory for measuring the Henry's Law constant for 1,2-epoxyhexane.

REFERENCES

1. Weijers, C. A. G. M., and de Bont, J. A. M. (1999) *J. Mol. Catal. B Enzym.* **6,** 199–214
2. Zou, J., Hallberg, B. M., Bergfors, T., Oesch, F., Arand, M., Mowbray, S. L., and Jones, T. A. (2000) *Structure* **8,** 111–122
3. Fretland, A. J., and Omiecinski, C. J. (2000) *Chem. Biol. Interact.* **129,** 41–59
4. Hernandez, O., and Bend, J. R. (1982) in *Metabolic Basis of Detoxification* (Jakoby, W. B., Bend, J. R., and Caldwell, J., eds) pp. 207–208, Academic Press, New York
5. Archelas, A., and Furstoss, R. (1998) *Trends Biotechnol.* **16,** 108–116
6. van Hylckama Vlieg, J. E. T., and Janssen, D. B. (2001) *J. Biotechnol.* **85,** 81–102
7. Faber, K., Mischitz, M., and Kroutil, W. (1996) *Acta Chem. Scand.* **50,** 249–258
8. Steinreiber, A., and Faber, K. (2001) *Curr. Opin. Biotechnol.* **12,** 552–558
9. Bradley, P. M., and Chapelle, F. H. (1998) *Environ. Sci. Technol.* **32,** 553–557
10. McCarty, P. L. (1997) *Science* **276,** 1521–1522
11. Henschler, D. (1994) *Angew. Chem. Int. Ed. Engl.* **33,** 1920–1935
12. Bolt, H. M., Lair, R. J., and Filser, J. G. (1982) *Biochem. Pharmacol.* **31,** 1–4
13. Carter, S. R., and Jewell, W. J. (1993) *Water Res.* **27,** 607–615
14. Magnuson, J. K., Stern, R. V., Gossett, J. M., Zinder, S. H., and Burris, D. R. (1998) *Appl. Environ. Microbiol.* **64,** 1270–1275
15. Newman, L. M., and Wackett, L. P. (1997) *J. Bacteriol.* **179,** 90–96
16. van Hylckama Vlieg, J. E. T., de Koning, W., and Janssen, D. B. (1996) *Appl. Environ. Microbiol.* **62,** 3304–3312
17. van Hylckama Vlieg, J. E. T., de Koning, W., and Janssen, D. B. (1997) *Appl. Environ. Microbiol.* **63,** 4961–4964
18. Yeager, C. M., Bottomley, P. J., and Arp, D. J. (2001) *Appl. Environ. Microbiol.* **67,** 2107–2115
19. Rui, L., Kwon, Y. M., Reardon, K. F., and Wood, T. K. (2004) *Environ. Microbiol.* **6,** 491–500
20. Shields, M. S., and Francesconi, S. C. (August 6, 1996) U. S. Patent 5,543,317
21. Shields, M. S., Montgomery, S. O., Chapman, P. J., Cuskey, S. M., and Pritchard, P. H. (1989) *Appl. Environ. Microbiol.* **55,** 1624–1629
22. Luu, P. P., Yung, C. W., Sun, A. K., and Wood, T. K. (1995) *Appl. Microbiol. Biotechnol.* **44,** 259–264
23. Nelson, M. J. K., Montgomery, S. O., O'Neill, E. J., and Pritchard, P. H. (1986) *Appl. Environ. Microbiol.* **52,** 383–384
24. Shields, M. S., Reagin, M. J., Gerger, R. R., Somerville, C., Schaubhut, R., Campbell, R., and Hu-Primmer, J. (1994) in *Bioremediation of Chlorinated and Polycyclic Aromatic Hydrocarbon Compounds* (Hinchee, R. E., Leeson, A., Semprini, L., and Ong, S. K., eds) pp. 50–65, Lewis Publishers, Boca Raton, FL
25. Shim, H., and Wood, T. K. (2000) *Biotechnol. Bioeng.* **70,** 693–698
26. Canada, K. A., Iwashita, S., Shim, H., and Wood, T. K. (2002) *J. Bacteriol.* **184,** 344–349
27. Vuilleumier, S. (1997) *J. Bacteriol.* **179,** 1431–1441
28. Jacobs, M. H., Van den Wijngaard, A. J., Pentenga, M., and Janssen, D. B. (1991) *Eur. J. Biochem.* **202,** 1217–1222
29. Visser, H., Bont, J. A. M. d., and Verdoes, J. C. (1999) *Appl. Environ. Microbiol.* **65,** 5459–5463
30. Visser, H., Vreugdenhil, S., Bont, J. A. M. d., and Verdoes, J. C. (2000) *Appl. Microbiol. Biotechnol.* **53,** 415–419
31. Misawa, E., Chion, C. K. C. K., Archer, I. V., Woodland, M. P., Zhou, N. Y., Carter, S. F., Widdowson, D. A., and Leak, D. J. (1998) *Eur. J. Biochem.* **253,** 173–183
32. Nakamura, T., Nagasawa, T., Yu, F., Watanabe, I., and Yamada, H. (1994) *Appl. Environ. Microbiol.* **60,** 4630–4633
33. Brannigan, J. A., and Wilkinson, A. J. (2002) *Nat. Rev. Mol. Cell. Biol.* **3,** 964–970
34. Stemmer, W. P. C. (1994) *Nature* **370,** 389–391
35. Rink, R., Fennema, M., Smids, M., Dehmel, U., and Janssen, D. B. (1997) *J. Biol. Chem.* **272,** 14650–14657
36. Nardini, M., Ridder, I. S., Rozeboom, H. J., Kalk, K. H., Rink, R., Janssen, D. B., and Dijkstra, B. W. (1999) *J. Biol. Chem.* **274,** 14579–14586

37. Nardini, M., Rink, R., Janssen, D. B., and Dijkstra, B. W. (2001) *J. Mol. Catal. B Enzym.* **11,** 1035–1042
38. Argiriadi, M. A., Morisseau, C., Hammock, B. D., and Christianson, D. W. (1999) *Proc. Natl. Acad. Sci. U. S. A.* **96,** 10637–10642
39. Franken, S. M., Rozeboom, H. J., Kalk, K. H., and Dijkstra, B. W. (1991) *EMBO J.* **10,** 1297–1302
40. Verschueren, K. H. G., Seljee, F., Rozeboom, H. J., Kalk, K. H., and Dijkstra, B. W. (1993) *Nature* **363,** 693–698
41. Sakamoto, T., Joern, J. M., Arisawa, A., and Arnold, F. H. (2001) *Appl. Environ. Microbiol.* **67,** 3882–3887
42. Gibson, T. J. (1984) *Studies on the Epstein-Barr Virus Genome.* Ph.D. thesis, Cambridge University, Cambridge, UK
43. Sambrook, J., Fritsch, E. F., and Maniatis, T. (1989) *Molecular Cloning: A Laboratory Manual*, 2nd Ed., Cold Spring Harbor Laboratory Press, Cold Spring Harbor, NY
44. Morales, V. M., Backman, A., and Bagdasarian, M. (1991) *Gene* **97,** 39–47
45. Baskaran, N., Kandpal, R. P., Bhargava, A. K., Glynn, M. W., Bale, A., and Weissman, S. M. (1996) *Genome Res.* **6,** 633–638
46. Dolfing, J., van den Wijngaard, A. J., and Janssen, D. B. (1993) *Biodegradation* **4,** 261–282
47. Spelberg, J. H. L., Rink, R., Kellogg, R. M., and Janssen, D. B. (1998) *Tetrahedron Asymmetry* **9,** 459–466
48. Sanger, F., Nicklen, S., and Coulson, A. R. (1977) *Proc. Natl. Acad. Sci. U. S. A.* **74,** 5463–5467
49. Rui, L., Kwon, Y. M., Fishman, A., Reardon, K. F., and Wood, T. K. (2004) *Appl. Environ. Microbiol.* **70,** 3246–3252
50. Schwede, T., Kopp, J., Guex, N., and Peitsch, M. C. (2003) *Nucleic Acids Res.* **31,** 3381–3385
51. Peitsch, M. C. (1993) *Bio/Technology* **13,** 658–660
52. Guex, N., and Peitsch, M. C. (1997) *Electrophoresis* **18,** 2714–2723
53. Rink, R., Kingma, J., Lutje Spelberg, J. H., and Janssen, D. B. (2000) *Biochemistry* **39,** 5600–5613
54. Perry, R. H., and Chilton, C. H. (1973) *Chemical Engineers' Handbook*, 5th Ed., pp. 3–39, McGraw-Hill Book Company, New York